Preliminary Design Report

Wichita State University

Team RISE

Rocket Inspiring Shocker Engineering

Tyrone Boswell – Propulsion and Trajectory
Mary Maneth – Aerodynamics
Fernanda Quezada – Structures
Amanda Smith – Stability and Control
Christina Wilson – Avionics and Recovery

Table of Contents

1. Executive Summary

Team RISE is an Aerospace Engineering senior design team that will be representing Wichita State University as the first competitive high-powered rocketry team from our university. The rocket design needs to meet the following two primary objectives for the mission: to achieve a large separation distance between booster and dart apogees, and to maximize dart apogee. To increase booster-dart separation distance, the team devised a drag chute on the booster portion of the rocket that would deploy upon dart separation. This drag chute consists of four “petals” that, when closed and secured under a small lip on the dart, form the transition section between the differing diameters of the dart and booster. At motor burnout, the differences in drag and change in acceleration causes the dart and booster to pull away from each other, releasing the petals and therefore dramatically increasing the drag experienced on the booster.

After performing aerodynamic and trajectory analyses to maximize the dart apogee distance, it was found that even a small increase in fuselage diameter and overall rocket weight decreased dart apogee significantly. In order to obtain minimal diameters and decrease structural weight for both the booster and the dart, Team RISE will develop custom-made aluminum mandrels for various structural aspects of the rocket: the nosecone, body tubes, boattail, transition/drag chute, couplers, and pistons. Using these mandrels, Team RISE will follow a procedure written by the team to lay-up a composite rocket structure using two plies of 5320-1/8HS, a pre-impregnated carbon fiber composite, and a layer of film adhesive. All composite lay-up will be performed by the team members at Wichita State University labs. Though there are challenges in laying up custom pieces, the payoff of doing so was found to far outweigh the risks: overall weight was decreased from 5.2 pounds to 3.7 pounds, and each section of the rocket’s cross-section has been minimized to minimally fit the internal payload. These two factors alone give the team a considerable competitive advantage.

Overall, the team was able to analyze the aerodynamic, structural, stability and control, propulsion and performance elements using basic engineering methods. Aerodynamic, stability, and control testing is being conducted in the Wichita State University 3x4 Wind Tunnel, while propulsion and structural testing will be performed in various aerospace laboratories. As this project is also being launched as part of the Aerospace Senior Design course, two launches will be performed in April—one a test launch and one a final launch for the course. The results of these launches have been predicted and will be discussed fully within the following report.

2. Scoring Analysis

A Kline-McKlintock sensitivity analysis was performed to determine the most important aspect of the competition (Miller). Several iterations were performed using values from Tripoli records and documented dart-rocket flights. In each iteration, the variables and their respective uncertainties were isolated individually to determine which variable has the largest impact. During all iterations, the apogee of the dart was the most sensitive except in the most extreme cases where uncertainties were either very high or very low. In general, the booster apogee was the next most sensitive criteria. This means the primary focus is achieving the highest possible altitude with the dart while making the booster apogee as low as possible.

3. Design Features of Rocket

3.1 Material Selection

Materials for initial consideration were selected according to what is available off-the-shelf (i.e. quantum, phenolic and HDPE) but weight was the most critical aspects to be optimized in order to improve the overall performance of the rocket. In order to reduce weight, research was conducted on composite materials. High strength, long fatigue life, low density, and adaptability are the major advantages of composite materials.

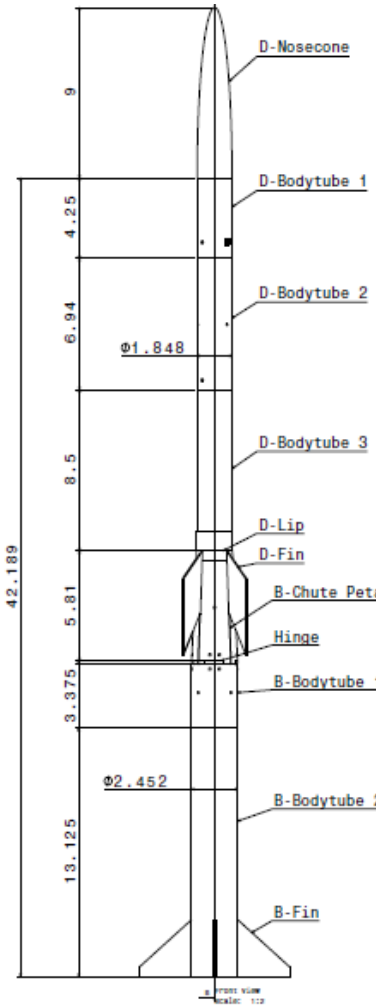

Figure 1. Overall rocket sizing and layout.

Body tubes, couplers, and pistons will be made out of two plies of 5320-1/8HS carbon fiber fabric and a layer of FM-300 film adhesive for a total thickness of 0.038 inches. Based on fin flutter requirements, dart fins will have a thickness of 0.07 inches and booster fins of 0.13 inches, corresponding to 5 and 10 carbon fiber plies.

3.2 Weight and Sizing

The overall rocket weight is 3.72 pounds, dart weight is 1.13 pounds and booster weight is 2.59 pounds. The rocket assembled together is 51.2 inches long, while the dart is 43.7 inches and the booster 22.5 inches (Figure 1).

Weight's Influence on Altitude

Since weight and drag oppose thrust, decreasing either force will result in a higher velocity and a higher altitude. A trade study regarding weight and its effect on altitude was performed in order to find out to which degree it affects the mission. The trade study found that the optimal weight was not necessarily a simple linear relationship. For the current drag coefficient, the optimal weight range for our rocket is between 1.5 and 4 pounds

(Figure 2). Our rocket weight is 3.72 pounds, which falls within the optimal range. The goal is to always decrease weight whenever possible.

Since this competition is unique (darts are not a common mission requirement), historical data is scarce and other teams' target altitudes are unknown.

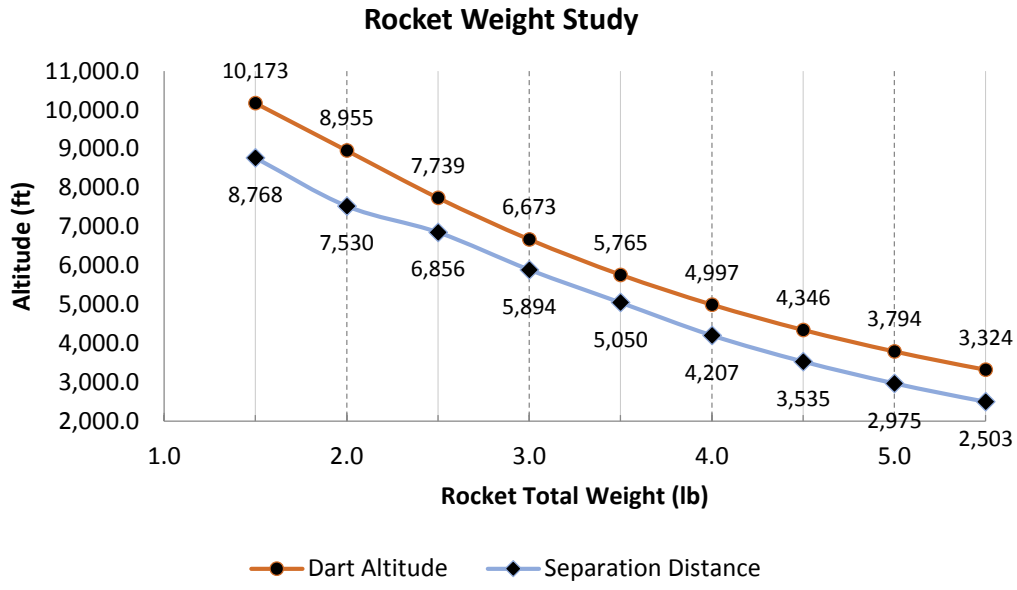

Figure 2. Rocket Weight Analysis. *Shows the relationship between total rocket weight versus both altitude and separation distance. (This performance is for a specific drag coefficient)*

Weight Distribution and Its Effect on Altitude

Another relationship is the effect of dart weight on altitude. The Dart Mass Ratio (DMR) is defined as the weight of the dart divided by the total vehicle weight. A trade study was performed to determine exactly how DMR affects the mission.

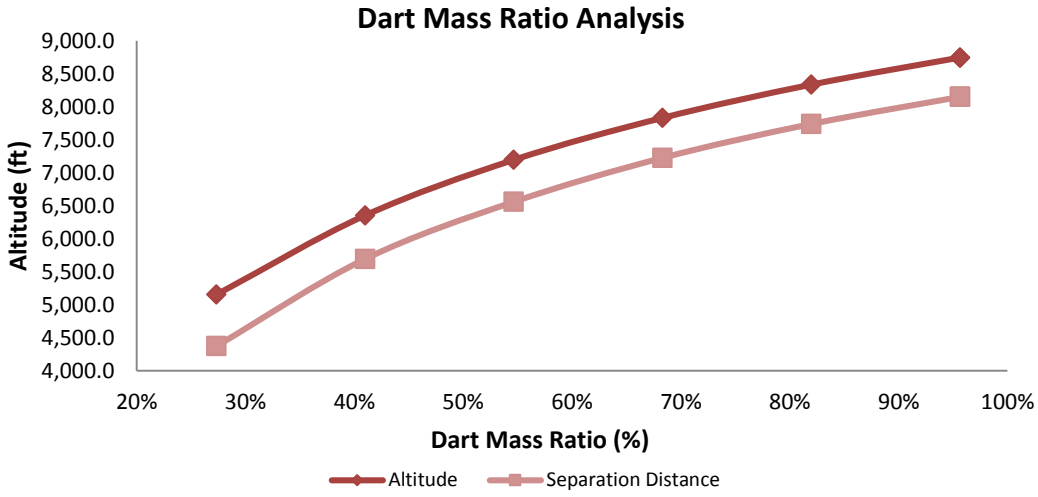

Figure 3. DMR Analysis. *Shows the relationship between DMR and both altitude and separation distance*

The results show a higher DMR gives a higher altitude. There is a similar relationship between DMR and the separation distance between the dart and the booster (Figure 3). From this, it would be prudent to decrease the total system weight while simultaneously putting most of the weight into the dart. Certain components are required to be within the booster (like the motor and the parachute) so there are physical constraints on DMR.

Results

The rocket weight is 3.72 pounds, dart weight is 1.13 pounds, and booster weight is 2.59 pounds. The maximum altitude of the dart is 5419 feet. The given $C_{D,min}$ for the booster is 11.06, the given dart $C_{D,min}$ is 0.25, and the given rocket $C_{D,min}$ is 0.58. The separation distance between the dart and the booster are 4661 feet. Maximum velocity is 606 mph and the maximum Mach number is 0.80.

3.2 Nosecone and Boattail

An elliptical nosecone shape was chosen after reviewing "Nose Cone and Fin Optimization" (Stroik) and *Topics in Advanced Model Rocketry* (Mandell); both documents suggest this contour if the flight is below 0.8 Mach. As explained under the Performance section, flight speeds are predicted to reach 0.81 Mach for 0.25 seconds. As this is only 1.6% of the ascent flight time, it was determined that the calculation could be attributed to error and that optimizing for subsonic flight is crucial.

The nosecone length was determined by taking into account fineness ratio-the ratio of the length of the nosecone to the base diameter-as well as critical Mach number. It is stated that a fineness ratio of 2 is "near optimum" (Mandell), but the fineness ratio was increased to keep the critical Mach number above predicted speeds. Ryan Felke's paper was used as a guide to incorporate compressibility effects in which he included Munk's Theory and a Karmen-Tsein Compressibility Correction (Felke). Using the elliptic contour chosen, the nosecone was determined to be 9 inches in length.

A conic boattail for the dart was also incorporated to reduce drag, specifically base drag. With no motor in the dart, the boattail comes to a point after 6 inches, theoretically eliminating base drag from the fuselage due to the gradual inclination.

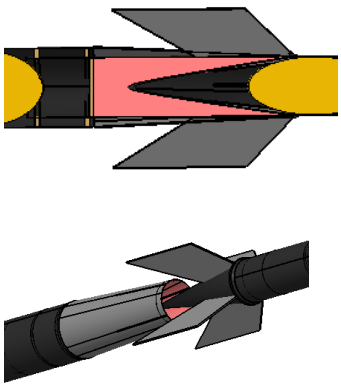

Figure 4. Cup-Like Structure (top) and Separated View (bottom).

3.3 Dart-Booster Connection and Drag Chute

The dart will be placed in the booster with a foam cup structure to hold it as seen in Figure 4. The length and surface contact of this structure is key to ensure adequate normal forces to secure the dart. During ascent, the thrust supplies more force than necessary to hold the rocket together. Since the thrust has a steep decline right before burnout, the forces continue to be significant enough until separation. Premature dart separation would only occur at severe angles of approximately more than 60 degrees from vertical.

From the scoring analysis, minimizing the booster apogee will improve the competition score. The easiest

way to accomplish this is to increase the drag on the booster immediately after separation. A drag chute device would increase the separation distance by roughly 49 percent, rationalizing the difficulty and risk involved with implementation.

The drag chute is designed to have four equal petals cut from a conic transition. Each petal is mounted to the booster with strap hinges. During ascent the petals are held closed by a lip structure on the dart. As the dart naturally separates from the booster, the drag petals will be released to a 90 degree angle with respect to the vertical. Bungee cord is connected from the cup assembly to each petal to ensure this angle and to create a smaller impulse during deployment. The drag chute assembly can be seen in Figure 5.

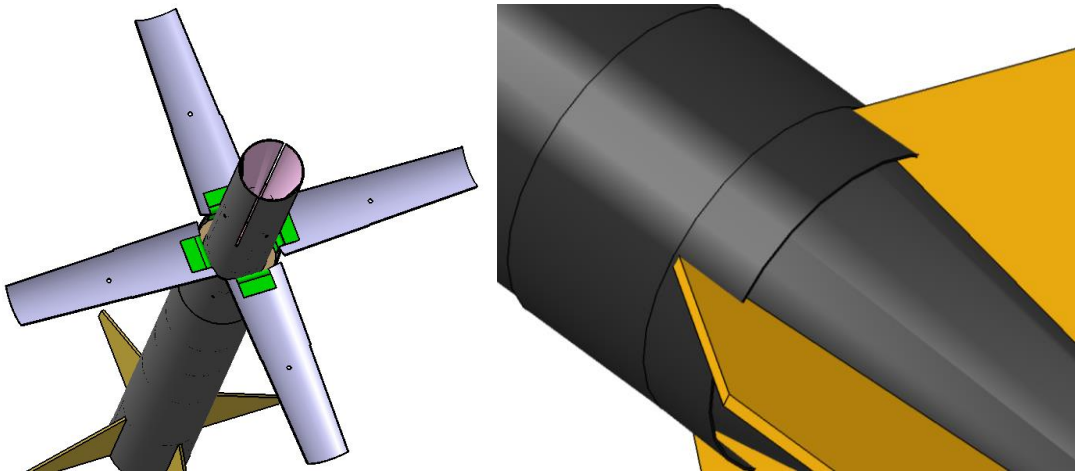

Figure 5. Fully Deployed Drag Chute (left) and Protective Lip for Drag Chute (right).

3.4 Recovery System

To ensure a safe descent rate of less than 20 feet per second, parachute selection was determined based off a simple calculation of descent velocity compared to parachute size. Setting the weight of the rocket equal to the drag force from the parachute, the following equation can be derived (Anderson): $v = \sqrt{\frac{2mg}{\rho C_{Dp} A_p}}$ where m is the mass of the respective assembly, and C_{DP} is the drag coefficient of the parachute which is estimated to be 1.38 (Hoerner). Table 1 shows the analysis to select the dart and booster parachutes.

	D_{out} (in)	D_{in} (in)	S (ft^2)	Mass (g)	Packed (in)	V (ft/s)	Impact (lbf)	Tug (lbf)
Dart	24	5	3.01	45.40	4.00	15.39	10.80	31.31
Booster	30	5	4.77	68.03	4.00	18.28	28.72	65.56

Table 1. Parachute analysis and selection.

The deployment method for the booster is a standard forward motor ejection charge. However, for the dart an aft electronic recovery deployment is being used. An Easy Mini altimeter will be used to safely eject the parachute after apogee using a preset altitude

setting. The altimeter will have an e-match connected to its main deployment terminals and running to a PVC pipe cap containing the ejection charge. This ejection system will be ground-tested prior to launch.

It was estimated that the shock cord length be three times the length of the rocket section (PML Recovery). Therefore, the length of shock cord for the dart is 104 inches and 68 inches for the booster. The shock cord chosen is 0.5625 inch thick tubular nylon. The packed space was estimated from PML's shock cord table, giving a packed length of 3.0 inches for the booster and 4.0 inches for the dart (PML Packing).

3.5 Propulsion System Specifications

The propulsion system features the Cesaroni I-445 motor as specified by the competition. The motor will sit inside of the default Cesaroni motor case for the I-445. To protect the carbon fiber from the harsh temperatures of the motor, the motor case will be placed snug within a Phenolic tube and then in the carbon fiber fuselage. The fins have curved tabs that allow them to slide in between the phenolic tube and the carbon fiber fuselage. The thrust curve used for trajectory calculations is shown in Figure 6 below.

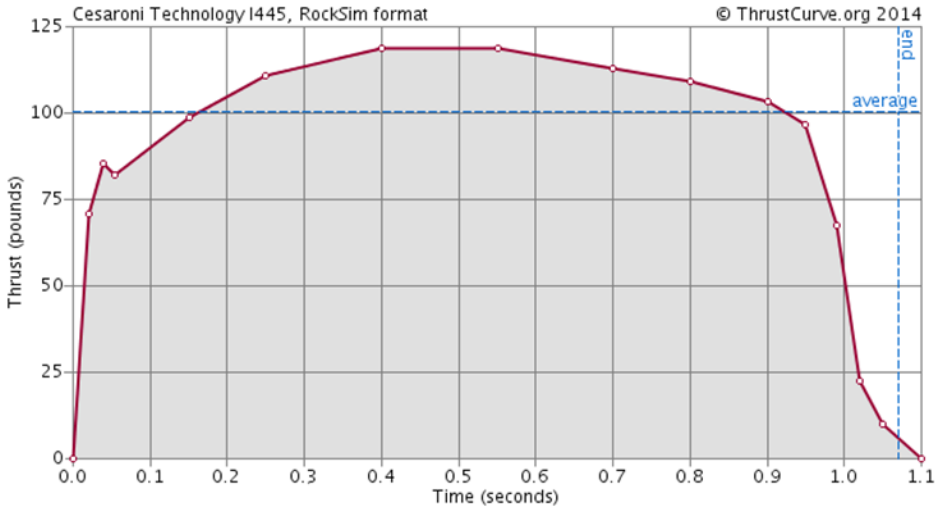

Figure 6. Thrust Curve. *This is the thrust curve as specified by www.thrustcurve.org*

4. Design Features of Payload

4.1 Avionic Components

To record the 3-axis rotation of the dart, a data collection system was designed using a 3-axis gyro sensor, an SD card and an Arduino Micro. The specific components were chosen based on the dart diameter of 1.8 inches and minimum weight. Each of these components are wired as seen in Figure 7 and the Arduino Micro will be programmed to log the data from the gyro sensor to the SD card.

A minimum of 1.5 hours run time for all electronics is required to power components from launch pad set up until landing with a possible delay from waiting for the next launch window. A pull pin switch allows conservation of power from assembly until

launch pad set up. A 400 mAh polymer lithium ion battery was selected to meet the required 193 mAhs.

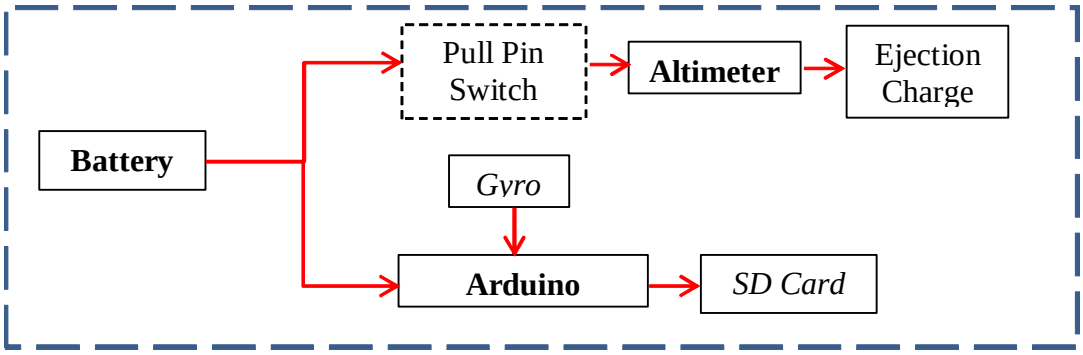

Figure 7. Dart Payload Schematic. *This shows the new payload components and their interactions with each other.*

The altimeter also needed to fit within the dart sizing limitations of 1.8 inch diameter and needed to be capable of deploying one parachute after apogee. It was chosen to be a small 1.5 by 0.8 inch Easy Mini Altimeter.

Other miscellaneous components needed in the dart include a tracker and pull pin switches. For safety reasons, switches are installed to prevent power supply to the ejection charge prior to being on the launch pad. The total weight of the dart payload is 0.22 pound-force. The booster payload contains only the competition altimeter.

4.2 Payload Configuration and Structure

The material chosen for the payload structure is 1/8 inch 3-Ply plywood since it provides sufficient strength and the team has access to a wood laser cutter on campus. The diameter of the dart needed to be minimized in order to decrease drag; therefore, the payload structure was designed to have a 1.8 inch inner diameter. As shown in Figure 8 the components are aligned in a row on one side of the bed in order to leave room for connections.

To ensure a down facing camera, the lens is installed on a shaft protruding out of the dart fuselage. This lens is from of a small purchasable key chain camera. The circuit board for the camera is installed on a payload bed within the rocket. In order to install the lens and camera circuit board the system needs to be independent from the remaining payload components which are placed aft of the camera since it contains the

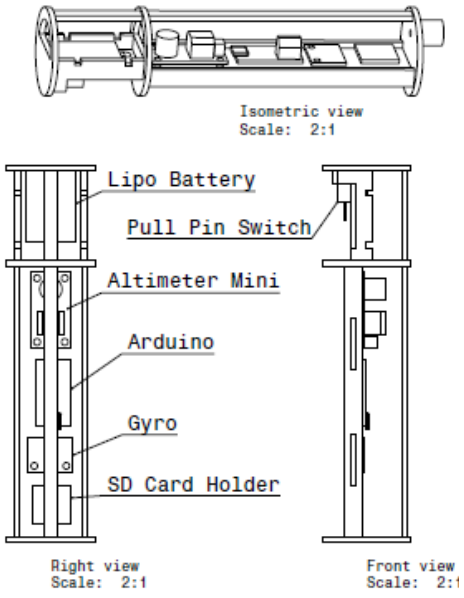

Figure 8. Dart Payload Structure and Layout.

rearward ejection charge. This can be seen in Figure 9. In addition, separation points in the body tube allow for installation of the avionics as well as parachute deployment.

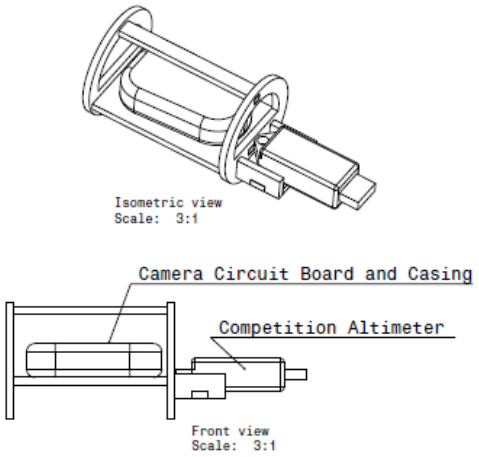

Figure 9. Camera Payload Structure and Layout.

5. Stability Analysis

Static stability is required during flight, and can help to minimize horizontal flight by keeping the rocket from deviating from vertical flight. The stability of the rocket requires positive zero-pitching moment coefficient and the negative pitching moment stiffness. The static margin or caliber is calculated taking the distance between the center of gravity (CG) and the center of pressure (CP), then dividing by the largest diameter.

A rocket with desirable stability will have a CG in front of the CP. A sufficient static margin is required because the rocket could generate large pitching moment stiffness, which creates a large damping ratio. A sufficient static margin results in reduction of dynamic oscillations and the short-period mode. In order to make this calculation, the location of the CG and CP must be known. For the center of gravity, CG, calculations, each individual component's mass was lumped at its CG and, assuming propellant mass to be constant, the CG locations of the rocket, dart and booster were calculated as follows (MIL-HDBK-762):

$$X_{CG} = \frac{\sum_{i=1}^{n} m_i x_i}{\sum_{i=1}^{n} m_i}$$

The distances from the nose of the dart to the CG of the rocket, the dart and the booster are 36.506 inches, 19.068 inches and 44.162 inches respectively.

The calculation of the CP was completed as discussed below, but with the following assumptions:

1. Flow over the rocket is potential flow (no vortices and friction)
2. The flow over the rocket is steady state and subsonic
3. Rocket is a rigid body
4. Axially symmetric
5. The angle of attack is very small (nearly zero)
6. Fins are thin plate

The rocket is divided into its separate section to obtain the theoretical center of pressure without great loss in the accuracy. The rocket is a combination of an elliptical nosecone, two cylindrical body tubes of two different diameters, a conic transition section, a boattail on the dart, four fins on the booster stage, and four fins on the dart. Each portion of the rocket has to be analyzed separately and the CP of each individual section must be calculated using the variables found in Figure 10. Then, the separate locations are combined together to obtain the final location of the CP.

d = diameter at base of nose	C_R = fin root chord
d_F = diameter at front of transition	C_T = fin tip chord
d_R = diameter at rear of transition	S = fin semi-span
L_T = length of transition	L_F = length of fin mid-chord line
X_P = distance from tip of nose to front of transition	R = radius of body at aft end
X_B = distance from nose tip to fin root chord leading edge	N = number of fins
X_R = distance between fin root leading edge and fin tip leading edge parallel to body	

Figure 10. Variables used within center of pressure calculations.

The CP of the nosecone was calculated by studying the method discussed in Barrowman's National Association of Rocketry Report. It is dependent on the body shape and volume. Using the Barrowman equations, the elliptical nosecone CP was found.

For the transition, the normal coefficient, $(C_N)_T$, and the CP location, X_T, of the transition were calculated using:

$$(C_N)_T = 2[(\frac{d_R}{d})^2 - (\frac{d_F}{d})^2] \quad \text{(Barrowman)}$$

$$X_T = X_p + \frac{L_T}{3}[1 + \frac{1-\frac{d_F}{d_R}}{1-(\frac{d_F}{d_R})^2}] \quad \text{(Barrowman)}$$

For the fins, fin flutter analysis had to be interpolated along with the CP calculations, as any change in fin geometry affects both quantities. Fin flutter largely impacts the performance of a rocket. If a rocket experiences fin flutter during its flight, altitude loss, loss of fins, and structural degradation can occur. To determine if the rocket would encounter flutter during flight, the speed at which the fin configuration would experience fin flutter was determined by considering the shear modulus of the material, G, fin thickness, t, semi-span, S, and root chord length to tip chord length ratio, λ. Using the equations given in the NACA technical note 4197 *Summary of Flutter Experiences as a Guide to the Preliminary Design of Lifting Surfaces on Missiles*, flutter velocity was determined using

$$V_f = a\sqrt{\frac{G}{\left[\left(\frac{(39.3)AR^3}{(\frac{t}{S})^3(AR+2)}\right)\left(\frac{\lambda+1}{2}\right)\left(\frac{P}{P_0}\right)\right]}} \quad \text{(NACA)}$$

From knowing when the fins flutter, this new fin geometry can be used to find the center of pressure. By interpolating these different values we were able to decrease the size of the fins, further cutting overall weight while still keeping in mind the stability criteria.

The fin center of pressure is located at the intersection of the quarter chord and the mean aerodynamic line, thus the normal coefficient of the fins, $(C_N)_F$, and CP location of the fins, X_F, is given by:

$$(C_N)_F = [1 + \frac{R}{S+R}][\frac{4N(\frac{S}{d})^2}{1+\sqrt{1+(\frac{2L_F}{C_R+C_T})^2}}] \quad \text{(Barrowman)}$$

$$X_F = \frac{X_t}{3}\frac{C_r+2C_t}{C_r+C_t} + \frac{1}{6}[C_r + C_t - \frac{C_r C_t}{C_r+C_t}] \quad \text{(Barrowman)}$$

The location of the CP of the entire rocket, X, is calculated using the normal coefficient of the overall rocket, $(C_N)_R$, equation:

$$(C_N)_R = (C_N)_{Nose} + (C_N)_T + (C_N)_{F_{booster}} + (C_N)_{F_{dart}} \quad \text{(Barrowman)}$$

$$X_{CP} = \frac{(C_N)_{Nose}X_N + (C_N)_T X_T + (C_N)_{F_{booster}}X_{F_{booster}} + (C_N)_{F_{dart}}X_{F_{dart}}}{(C_N)_R} \quad \text{(Barrowman)}$$

These equations result in an overall rocket CP location of 40.1 inches from the nose tip.

After determining the location of the CP and the location of the CG the caliber can be calculated. This caliber is 1.5. This is a reasonable value for the caliber because it is a rule of thumb based on years of experience in model rocketry that the stability caliber be greater than one.

Another important aspect of the rocket is that, when separated from the overall assembly, the dart and booster must also be stable on their own. For this, the same equations from above were used to determine the CP of the dart and booster separately. This resulted in a CP location of 22.03 inches from the nose tip for the dart, and 20.95 inches from the top of the booster with drag chute deployed. When compared to the calculated CG, we get a stability caliber of 1.6 for the dart and 2.1 for the booster. Figure 11 shows the CG and CP locations of the assembled rocket, dart, booster with closed drag chute and booster with deployed drag chute. A summary of these values can be found in Table 2.

	Rocket	**Dart**	**Booster (Open Drag Chute)**
Center of Pressure	40.10 inches	22.03 inches	20.95 inches
Center of Gravity	36.54 inches	19.04 inches	15.71 inches
Stability Caliber	1.5	1.6	2.1

Table 2. Stability Parameters.

After taking into consideration fin flutter, fin material, and CP calculations, the new fin configurations are as followed: for the dart, there are 4 fins of root chord 3 inches, tip chord 4 inches, sweep length 1.5 inches, semi-span 1.4 inches, and a thickness of 0.07 inches; for the booster, there are 4 fins of root chord 3 inches, tip chord 0.5 inches, sweep length 2.5 inches, semi-span 2.8 inches, and a thickness of 0.13 inches. This gives us a critical flutter velocity of 6,536 mph for the dart fins and 1,266 mph for the booster fins. As referenced earlier, the maximum velocity is 622 mph, meaning that the fins will not experience flutter at any point throughout flight duration.

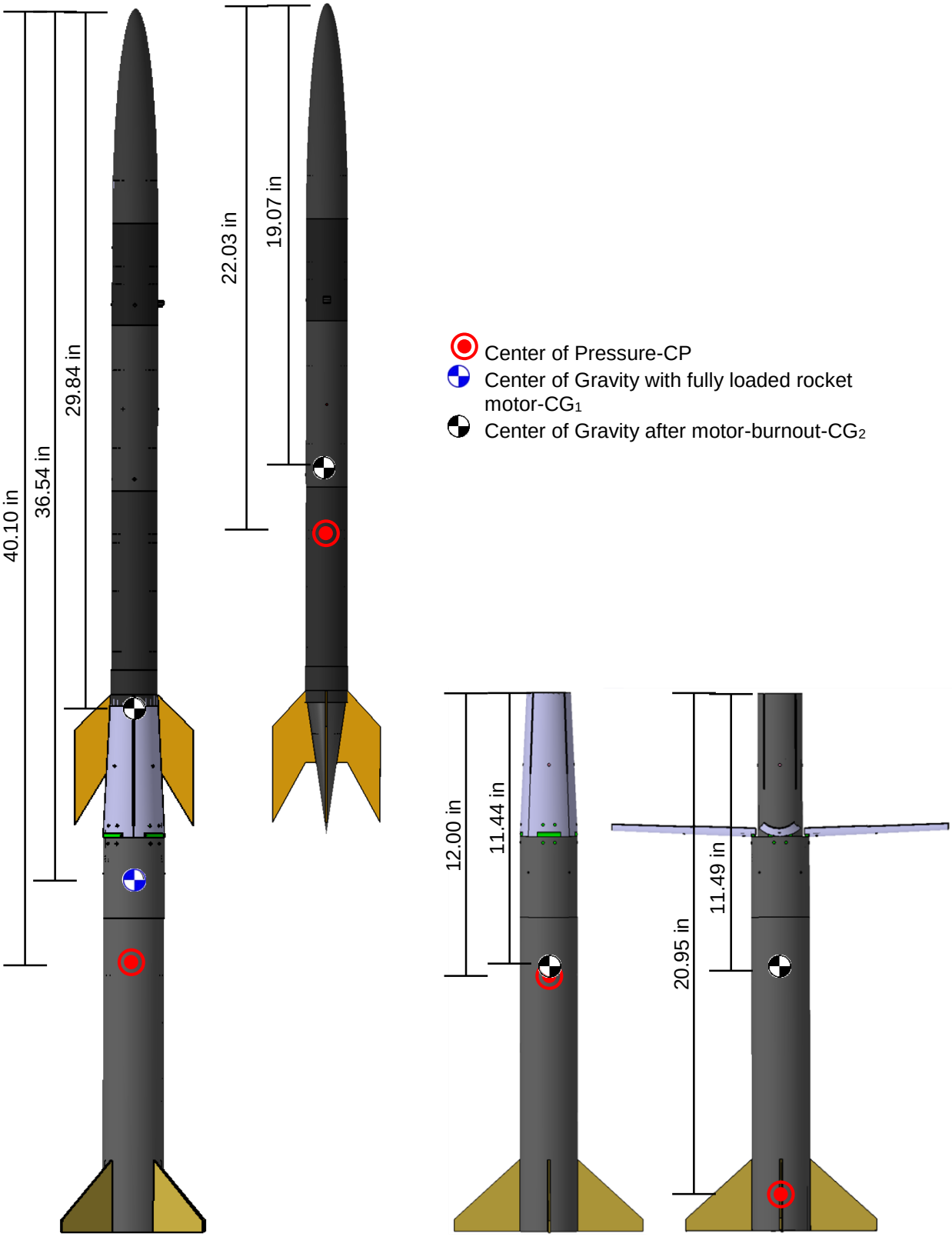

Figure 11. CP and CG locations for assemblies.

6. Structural Analysis

Structural analysis on the main load path of the rocket (i.e. body tubes) was performed assuming constant fuel, vertical (i.e. zero-angle of attack) and no wind gusts.

6.1 Axial Loads

Since the primary source of axial loads is the thrust of the motor, axial load analysis was performed at 0.4 seconds, when the maximum thrust experienced is 118 pounds. The axial force at several stations along the fuselage was calculated (Hibbeler); the largest loads suffered by the fuselage occur at the engine bulkhead as seen in Figure 12.

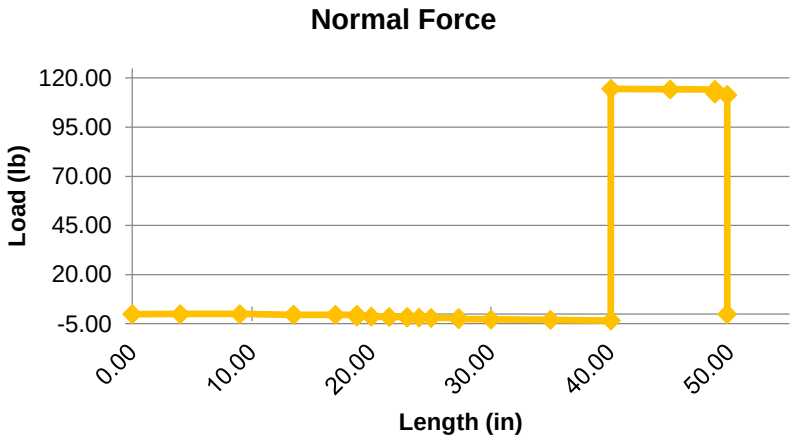

Figure 12. Axial Force Diagram. *Highest loads occur at the propulsion bulkhead.*

6.2 Pressure

The normal stress in the hoop and longitudinal directions were calculated treating the rocket as a thin-wall pressure vessel ($\frac{r}{t} > 10$). Worst-case pressure loads occur at apogee since the pressure differential inside and outside of the rocket is the largest. Simplifying the fuselage as cylindrical vessels and the nose cone and boattail as a cones the following equations were used:

Cylindrical Vessels (Hibbeler): $\sigma_1 = \frac{pr}{t}$ $\sigma_2 = \frac{pr}{2t}$ Cone (Roark): $\sigma_1 = \frac{pr}{tcos\alpha}$ $\sigma_2 = \frac{pr}{2tcos\alpha}$

After applying a safety factor of 1.5, stress values are considerably lower than the material's yield stress. Detailed results of the analysis can be seen in Table 3 where actual Wichita altitude was considered.

Component	Apogee altitude (ft)	P_{gauge} at apogee (psi)	Design $\sigma_1 < F_{1t}$		Design $\sigma_2 < F_{12}$		Design $\tau_2 < F_6$	
			Design σ_1 (psi)	Actual FS	Design σ_2 (psi)	Actual FS	Design τ_2 (psi)	Actual FS
Dart Body Tube	6990	6990	482.42	290.20	241.21	514.07	241.21	42.70
Nose Cose	6990	2.68	246.50	567.96	123.25	1006.11	123.25	83.57
Boattail	6990	2.68	248.07	564.37	124.03	999.73	124.03	83.04
Booster Body Tube	2043	0.38	89.34	1567.01	44.67	2775.84	44.67	230.57

Table 3. Pressure Vessel Analysis. *Analysis was done at the respective apogees of the dart and the booster.*

6.3 Buckling

To analyze buckling the rocket was divided into five bays at the location of bulkheads. Critical stresses were calculated at the base during highest thrust with the following formulas (Hibbeler):

$$P_{cr} = \frac{\pi^2 EI}{L^2} \qquad \sigma_{cr} = \frac{P_{cr}}{A_{cross\ section}}.$$

Results in Table 4 show that the critical stresses and loads are lower than the composite material strength, indicating that no buckling will occur. The propulsion bay is the most critical location.

Structure	Stress (psi)	Material's critical stress (psi)	Buckling?
Nose cone	36.59	7377.05	No
Dart body tube	32.81	7377.05	No
Boattail	32.27	7377.05	No
Booster body tube	15.53	5648.54	No

Table 4. *Buckling analysis results*

6.4 Payload Bed Analysis

In order to ensure safe flight the structural integrity of the different plywood payload beds was analyzed. Calculations were done assuming worst-case scenario to be vertical flight when the rocket experiences maximum loading (i.e. 35 g's at maximum thrust). Analysis results demonstrating no failure can be seen in Table 5.

Structure Bed	Component	Weight (lb)	Loading * Weight (lb)	Area (in^2)	Stress (psi)	Design Stress (psi) [assuming 1.5 FS]	Birch Plywood Shear Strength (psi)	Failure
Battery	Battery	0.020	0.694	2.545	0.273	0.409	401.750	None
Electronics	Arduino	0.004	0.140	2.545	0.055	0.083	401.750	None
	Altimeter	0.014	0.502	2.545	0.197	0.296		
	Gyro/sensor	0.007	0.247	2.545	0.097	0.146		
	SD Card	0.007	0.231	2.545	0.091	0.136		
					Total	0.66		
Camera	Camera	0.031	1.080	2.545	0.425	0.637	401.750	None

Table 5. *Structural Payload Bed Analysis.* Vertical flight at 35 g's.

7. Performance Analysis

7.1 Launch / Flight Analysis

The heart of the trajectory analysis is the free body diagram, which features a thrust vector, opposed by the weight and drag vectors. This net force is calculated using the thrust curve (Figure 6) and the weight of the rocket. The consumption of propellant mass is assumed to be constant. Drag is calculated using the minimum drag coefficients for the rocket, dart, and booster. Velocity comes from the net force, and drag comes from velocity so an iterative exchange with the aerodynamic analysis is used to pinpoint the correct values for drag. Acceleration is based on the net force and altitude is based on velocity, *v,* and time *t.*

$$\text{Velocity: } v_1(t) = v_o + \frac{F_1 + F_o}{2} * \frac{t_1 - t_o}{\frac{W_1}{g_0}}$$

$$\text{Altitude: } h_1(t) = h_o + v_1(t_1 - t_o)$$

$$\text{Total Force: } F_1 = T_1 - D_1 - W_1$$

Optimal separation occurs when there is no friction or interference between the dart and the booster; therefore, the two sections of the rocket should have minimal interaction. Referencing the force equation above, the burn phase has thrust opposing the drag and the weight vectors. During coast, that thrust is no longer occurring and is completely opposed by drag and weight. At this point, the dart's altitude is completely dependent on minimizing these two opposing forces. Graphs of the rocket velocity, rocket acceleration, and dart velocity are shown in Figures 13, 14 and 15.

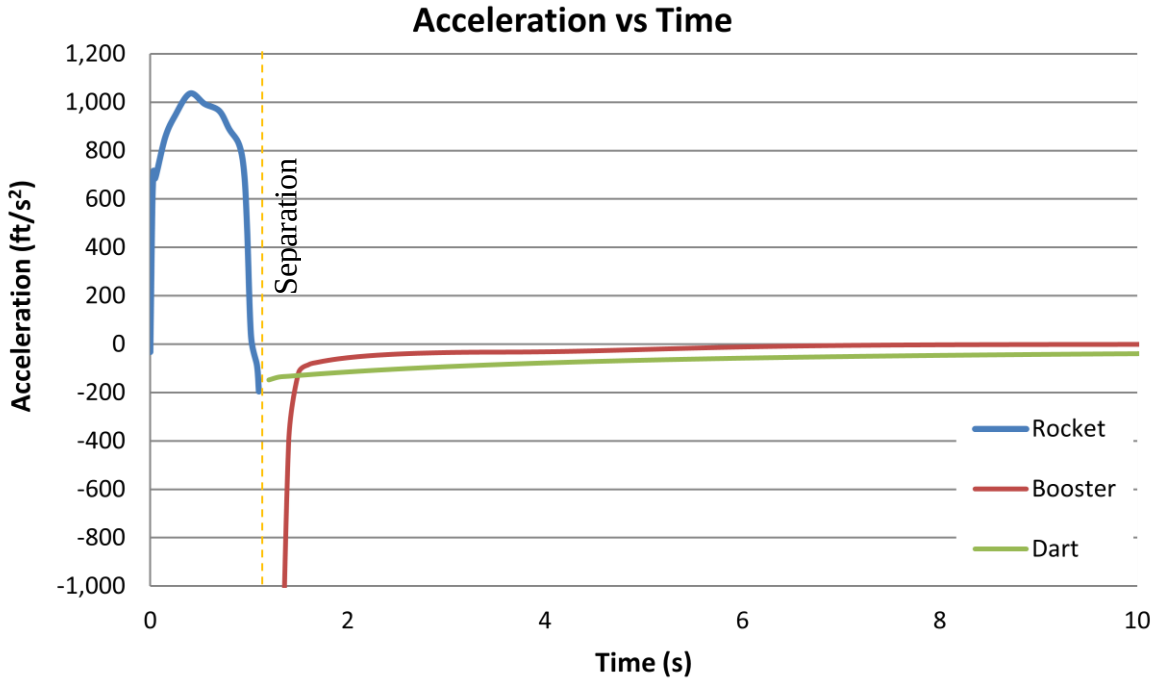

Figure 13. Total Acceleration vs Time. *This shows the change in acceleration for the entire flight.*

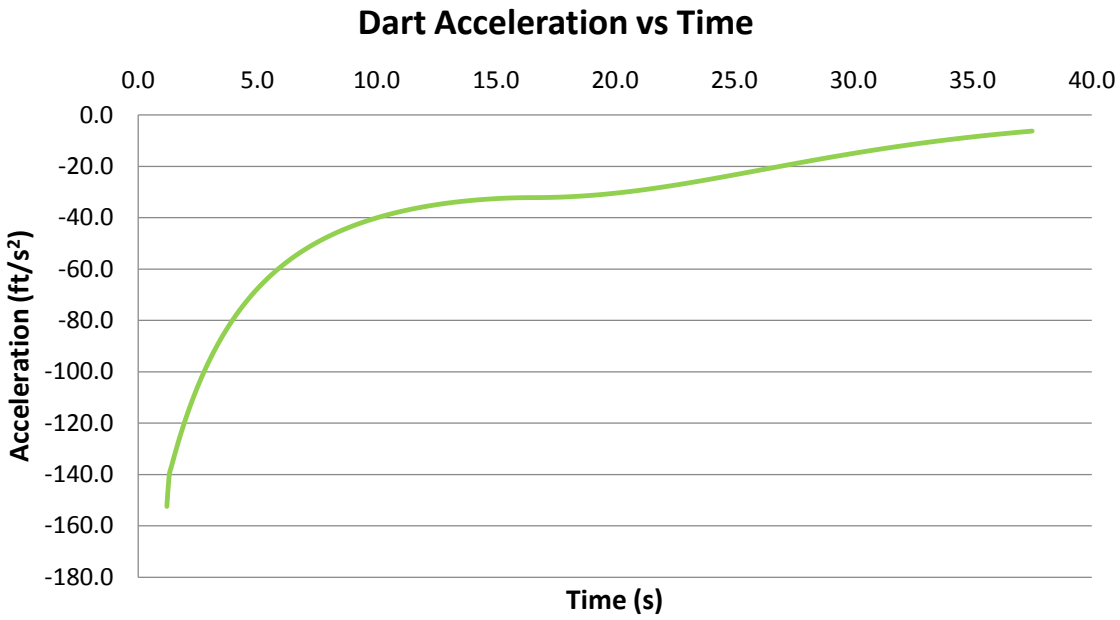

Figure 14. Dart Acceleration vs Time. *This shows the change in dart acceleration after separation.*

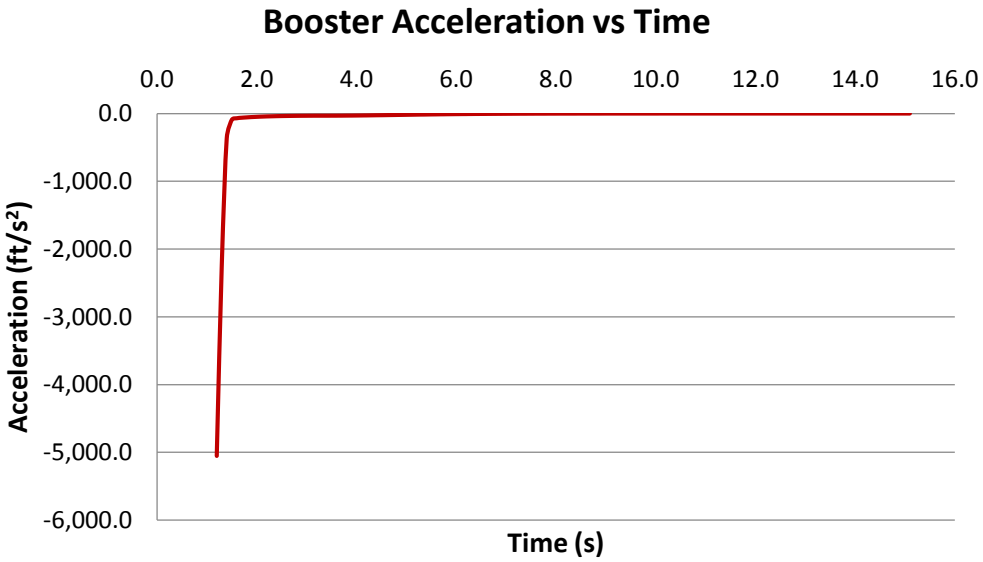

Figure 15. Booster Acceleration vs Time. *This shows the change in booster acceleration after separation. Please note that this is with the drag chute deployed.*

7.2 Drag Predictions

Drag coefficients for each assembly were determined by performing a component build-up. Each component was isolated wherein each type of drag was determined along with the appropriate reference area. The components for each assembly can be seen in Table 6. The types of drag a component was evaluated for are wave drag, friction drag, and base drag.

Rocket	Dart	Booster
Elliptic Nosecone	Elliptic Nosecone	Hollow Nose
Dart Body	Dart Body	Cup Body
Dart Fins	Dart Fins	Drag Petals
Transition	Boattail	Booster Body
Booster Body		Booster Fins
Booster Fins		Base
Base		

Table 6. Component Breakdown of Assemblies.

Wave drag and base drag coefficients were found using experimental from military handbook "Design of Aerodynamically Free Stabilized Rockets" (MIL-HDBK) and Hoerner's *Fluid Dynamic* Drag (Hoerner). These values were assumed to be constant during flight even though they technically change with speed. With experimental data, interpolation was sometimes necessary as was using data for a similar scenario when the exact case could not be found; when this happened, drag was typically overestimated as an attempt to not falsely overestimate performance. The reference area was the respective projected area.

Friction drag was calculated for each component except for the base, front of the cup, and drag petals. Friction drag was determined base off of Reynold's number, Re, where

$$Re = \frac{\rho v l}{\mu} \text{ (Anderson)}$$

After finding the transition from laminar to turbulent flow happened near the tip of the rocket, it was fair to assume the entirety of flow was turbulent. Therefore, the friction coefficient for each part was found using Raymer's equation for a flat plate:

$$C_f = \frac{0.455}{(log_{10} Re)^{2.58}(1+0.144M^2)^{0.65}} \text{ (Raymer)}$$

A correction factor of 15% was added to all circular components like the nosecone and fuselage (MIL-HDBK). The reference area used for friction drag was the wetted area of each respective component.

Once each component's drag coefficients were calculated, the total drag of that component was calculated using

$$D = \frac{1}{2}\rho v^2 s c_D \text{ (Anderson)}$$

and finally the overall drags of each component were then totaled to find the overall drag of each assembly. This was done at each time step as the velocity changed. The drag coefficient of each assembly was then found with respect to the projected area of the fuselage. This was an iterative process with propulsion data where drag values

were used to determine velocities and then velocities were used to determine drag values until they matched. It was then found that the number of iterations could be greatly reduced to simply find the minimum drag coefficient of each assembly, and that be used as a constant for altitude predictions. The drag coefficients for each assembly can be found in Table 7.

Assembly	Minimum Drag Coefficient
Rocket	0.584
Dart	0.246
Booster	11.06

Table 7. Minimum Drag Coefficients of Different Assemblies.

7.3 Altitude Predictions

The dart and booster apogee predictions as well as the maximum velocity predicted to be attained by the rocket are summarized in Table 8.

As discussed in the Weight and Sizing section, there is an important relationship between altitude performance and weight. Figure 16 shows the relationship between DMR, total rocket weight and altitude.

Booster Max Altitude (ft)	757.9
Dart Max Altitude (ft)	5,418.7
Dart & Booster Separation (ft)	4660.8
Max Velocity (ft/s)	888.6
Mach number	0.80
Max Acceleration (ft/s^2) – Rocket (post separation)	1054.0
Max Acceleration (ft/s^2) - Booster	-4,765.6
Max Acceleration (ft/s^2) - Dart	-148.3

Table 8. Altitude and velocity predictions.

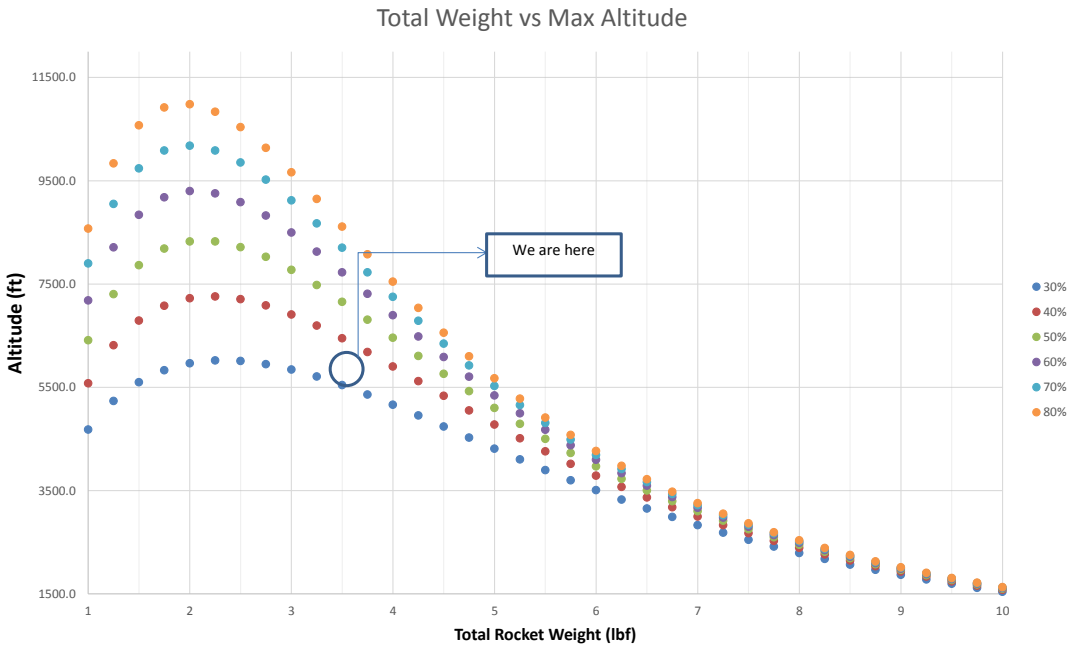

Figure 16. Optimal Weight Trade Study. *This shows the relationship between DMR, total rocket weight, and altitude given the rocket's configuration.*

8. Construction and Assembly Process

All construction and assembly will be performed by the team members. The team received mentoring and advice from professors and machine shop staff. This section includes construction of mandrels, laying up composites, machining and cutting materials, assembling overall rocket and payload, and assembly during launch day.

8.1 Mandrel Construction

Figure 17. Stair-step patter for initial cutting of complex curves.

All mandrels were lathed from solid T6061 Aluminum bars. Cylindrical lathes for pieces like body tubes, pistons, couplers, etc. were machined on a manual lathe. Under the guidance of the lab supervisor, the proper spindle speed was found to acquire the appropriate surface speed of the material, as well as a good feed rate for cutting tool. All pieces had to be supported by a live center. The final size and surface finish was acquired by running the final cut multiple times as well as using 400 grit sandpaper.

Mandrels for complex shapes such as the nosecone, boattail, lip, drag chute petals, etc., were machined on a CNC lathe. While 3D software like CATIA and MasterCam was helpful in determining the points, the actual code for the lathe was simply using the correct vernacular in Notepad. For straight tapers like the boattail and lip, the coding for the machine was rather simple since the tool can be programmed to follow the straight line after an initial stair-step pattern for cutting away the initial excess as seen in Figure 17. The curves for the ellipse on the nosecone and its respective coupler also started with an initial stair-step pattern, and the actual curve was simulated by multitudes of straight lines. If the surface finish was not already acceptable, 400 grit sandpaper was used to smooth any irregularities.

8.2 Composite Layup

Patterns for the dart and booster body tubes, couplers and pistons will be cut out of carbon fiber and film adhesive. All mandrels will be covered with release agent and a release film layer. Next, the carbon fiber patter plies will be laid-up on the mandrels and topped with the film adhesive. Each piece will be vacuum-bagged and placed in the oven at 250 ±10°F for approximately five hours.

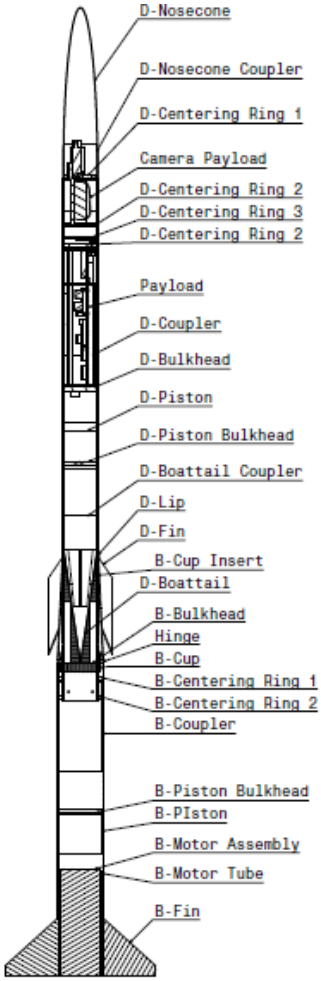

Figure 18. Overall rocket assembly.

A flat surface covered with a release film will be used to lay up the dart and booster fins. On top of the release film, five plies and ten plies of carbon fiber will be laid-up for the dart and booster fins respectively and covered with another release film. Afterwards, the mandrels will be vacuum-bagged and placed in the over at 250 ±10°F for five hours. Fins will be then cut using a water-jet cutter.

8.3 Overall Assembly

Following mandrel and composite layup of structural pieces is the overall assembly of the rocket. This construction will be performed in the safety of the on campus rocket lab and work will not be done alone for safety reasons. The fuselage pieces, couplers, pistons, bulkheads will be assembled using epoxy in the order written in an instruction manual created by the team and as seen in the overall rocket assembly Figure 18. The payload structure will also be assembled using epoxy and electronics will be installed on the payload bed using screws and zip ties as specified in the team manual. Pressure holes will be drilled after full assembly of the dart to ensure alignment. To construct the drag chute system, first the cup structure must be installed within the booster using centering rings. Following this, the hinges are attached with screws extruding from the outside of the fuselage into the cup structure. This alignment is critical. The bungee cord must then be installed first within the cup then onto each petal. After full structural construction of the dart and the booster, the payload and parachute can be inserted. Lastly, the dart is aligned and placed within the booster for complete rocket assembly.

9. Launch Day Procedures

9.1 Safety and Handling Procedures

Safety is a high priority for the team. During layup of the composites and the fabrication of the mandrels, there was supervision by staff during each session. The composites lab was cleaned before and after each layup to minimize exposure and contamination of the product. The motors were placed in a fire-proof, blast-proof safe prior to use. Regarding transportation, the team plans to transport the rocket to Minnesota via car. The rocket will be mostly assembled, though the two stages may be separated and the drag chute secured to prevent unwanted deployment. The motor shall be placed in a safe container to prevent unintended ignition.

9.2 Pre-Launch Procedures

The camera payload bed and the avionics payload beds will be installed in the dart along with the ejection charge. A remove-before-launch pin will be inserted into the rocket for safety prior to launch. Following this, the motor shall be assembled into its motor case and placed into the aft section of the booster. After obtaining and activating the competition altimeters, they shall be placed into the payload section of the dart and the bottom of the cup structure in the booster. An e-match will be inserted into the rocket motor once the rocket is in place on the launch pad. Lastly, the remove before launch pin will be removed and team will listen for sound to ensure the payload system is on.

9.3 Post-Launch Procedures

Tracking will be used to find the rocket upon landing. Immediately after finding the components of the rocket, the payload will be turned off and the team will return to the launch site. The motor will be removed and the data will be taken off of the electronics and placed onto a laptop.

10. Budget

Type	Component	Quantity	Unit Cost	Cost
Structure	1/8 in Plywood	1	$4.59	$4.59
Structure	Carbon fiber (5320-1/8HS)			Donated
Structure	Film adhesive (FM-300)			Donated
Layup	2.5 in & 2 in aluminum rods	49 in		$160.00
Layup	Vacuum bags, breather and release film			Donated
Electronic Payload	Dart Radio Tracking System			Donated
Electronic Payload	Battery (Lithium)	1	$6.95	$6.95
Electronic Payload	Lipo Battery Charger	1	$14.95	$14.95
Electronic Payload	Switch & Wires			$4.69
Electronic Payload	Arduino	1	$19.95	$19.95
Electronic Payload	Micro USB Cable	1	$4.95	$4.95
Electronic Payload	Gyro/sensor	1	$49.95	$49.95
Electronic Payload	SD Card & Holder	1	$9.95	$15.47
Electronic Payload	Camera	1	$45.99	$45.99
Electronic Payload	Altimeter (Easy Mini)	1	$85.60	$85.60
Electronic Payload	Altimeter 2 (Competition)	2	$69.95	$139.90
Propulsion	Motor	1	$52.99	$52.99
Propulsion	Motor casing & closure	1	$85.50	$85.50
Recovery	Black Powder & ejection charge container			$20.38
Recovery	Shock chord (Dart & Booster)	5	$1.99	$9.95
Recovery	Parachutes	2	$23.62	$47.24
Structure	Pink insulation foam			Donated
Drag Chute	Bungee chord	150 ft		$24.00
Structure	Sandpaper			Donated
Structure	Phenolic Motor Tube	1	$7.00	$7.00
Structure	Epoxy	5	$5.29	$26.45
Propulsion	Launch Buttons & E-Matches			$19.00
Hardware	Screws, hinges, etc.			$38.00
Competition	Registration	1	$400.00	$400.00
Competition	Hotel (2 rooms, 3 nights)	6	$89.00	$534.00
Competition	Transportation	4	$524.00	$2,096.00
			Total	**$ 3,913.50**

References

"2014-2015 NASA's Space Grant Midwest High-Power Rocket Competition Handbook," Minnesota Space Grant Consortium, August 2014, URL: aem.umn.edu/mnsgc/space_grant_midwest_rocketry_competition_2014_2015 [cited 5 November 2014]

Anderson, J.D., Introduction to Flight. McGraw-Hill, 7th ed., New York, 2005.

Barrowman, James S., Judith A., "The Theoretical Prediction of the Center of Pressure, Research and Development Project NARAM-8."

Dameräu, D., "Axial Tubes Crush Tests", *High Power Rocketry Strength of Materials*, URL: http://www.rocketmaterials.org/datastore/tubes/Axial/index.php [cited 2 November 2014] Table 6.3.1

Felke, R. J., "Effect of Different Nose Profiles on Subsonic Pressure Coefficients," Rocket Science and Engineering Technologies.

Hibbeler, R. C. Mechanics of Materials,13th ed., 5th ed., Prentice Hall, Upper Saddle River, NJ, 1997, pp. 406, 464-475, and 657-664.

Hoerner S. F., Fluid-Dynamic Drag, Great Britain, 1992

Martin, Denis J., Summary of Flutter Experiences as a Guide to the Preliminary Design of Lifting Surfaces on Missiles, NACA TN-4197, Langley Aeronautical Laboratory, Langley Field, Va, February 1958.

MIL-HDBK-762: "Design of Aerodynamically Stabilized Free Rockets", Department of Defense, 1990.

Miller, S., PhD, "Competition Uncertainty & Sensitivity Analysis Example," Lecture. AE 528. Wichita State University. Blackboard. Web. 10 Sept. 2014.

Mandell, G. K., Caporaso, G. J., and Bengen, W. P., Topics in Advanced Model Rocketry, MIT Press, Massachusetts Institute of Technology, Cambridge, MA, 1973, Chap. 3.

Public Missiles Ltd, "PML Chute Packing Space Requirements & PML Tubular Nylon Packing Space Requirements," URL: https://publicmissiles.com/ [cited November 5, 2014]

Public Missiles Ltd, "PML Recovery Components FAQ," URL: https://publicmissiles.com/ [cited November 5, 2014]

Raymer, D. P., "Aircraft Design: A Conceptual Approach."

Roark, R.J and W. C. Young, *Formulas for Stress and Strain,* Fifth Edition, McGraw-Hill Book Company, Inc., NY, 1975, Chapter 13, pp. 445-512.

Sampo Niskanen and others, OpenRocket, Model Rocket Simulator Software, Ver. 13.11, 2007.

Stroik, G., "Nose Cone & Fin Optimization," Tripoli, Minnesota, 2011 (unpublished).

Tripoli Rocketry Association, Inc, "Code for High Power Rocketry Tripoli Rocketry Association," URL: http://www.tripoli.org/ [cited November 5, 2014]